DOI: 10.1021/cg901100z

CRYSTAL GROWTH & DESIGN Article

2009, Vol. 9
5356–5362

Structural Isomerism of Luminescent Dinuclear Pt(II)-Thiolate Diimines

Biing-Chiau Tzeng,*,† Tse-Hao Chiu,† Sun-Yi Lin,† Chieh-Min Yang,† Tsung-Yi Chang,† Cyong-Huei Huang,‡ A. Hsiu-Hua Chang,‡ and Gene-Hsiang Lee§

†*Department of Chemistry and Biochemistry, National Chung Cheng University, 168 University Road, Min-Hsiung, Chiayi 62102, Taiwan,* ‡*Department of Chemistry, National Dong Hwa University, Shoufeng, Hualien 97401, Taiwan, and* §*Department of Chemistry, National Taiwan University, 1, Sec. 4, Roosevelt Road, Taipei 10617, Taiwan*

Received September 9, 2009; Revised Manuscript Received October 15, 2009

ABSTRACT: An efficient method has been developed to isolate a series of *anti* and *syn* isomers of dinuclear Pt(II)-thiolate diimines, *anti*-[Pt(d-*t*-bpy)(NS_2)]$_2$(ClO_4)$_2$ (**1a**), *syn*-[Pt(d-*t*-bpy)(NS_2)]$_2$(ClO_4)$_2$ (**1b**), *anti*-[Pt(d-*t*-bpy)(N_2S)]$_2$(PF_6)$_2$ (**2a**), *syn*-[Pt(d-*t*-bpy)(N_2S)]$_2$(ClO_4)$_2$ (**2b**), and *syn*-[Pt(d-*t*-bpy)(NOS)]$_2$(ClO_4)$_2$ (**3**) (d-*t*-bpy = 4,4′-di-*tert*-butyl-2,2′-bipyridine, HNS_2 = 2-mercaptobenzothiazol, HN_2S = 2-mercaptobenzimidazol, HNOS = 2-mercaptobenzoxazol). In fact, it provides a rational strategy to isolate a series of *anti* and *syn* isomers of dinuclear Pt(II) thiolates, where the *syn* isomers all show intermolecular Pt(II)···Pt(II) contacts of 3.510(4)−3.859(4) Å. To examine the correlation between the luminescence and intermolecular Pt(II)···Pt(II) contacts, solid-state luminescence measurements of the dinuclear complexes at room temperature and at 77 K have been carried out. Indeed, there is no obvious correlation between their emission energies and intermolecular Pt(II)···Pt(II) interactions, although our theoretical calculations suggest that these interactions are involved in their excited states. However, the dinuclear complexes with larger red-shifts of 1260 (**1b**) and 840 cm^{-1} (**2b**) are in parallel with their increased intermolecular $\pi\cdots\pi$ interactions. In addition, the glass luminescence at 77 K and their concentration-dependence measurements conducted for **1a** and **1b** further support that intermolecular $\pi\cdots\pi$ interactions instead of Pt(II)···Pt(II) ones are most likely correlated with the solid-state luminescence.

Introduction

Studies have revealed that some square-planar d^8-metal complexes have a strong tendency to stack in the solid state and show characteristic optical and electrical properties.[1] The stabilization of these structures is attributed in part to bonding interactions arising from the overlap of the $5d_{z^2}$ and $6p_z$ orbitals of adjacent metal centers, leading to dσ (dσ*) and pσ (pσ*). Configuration interaction (CI)[2] with the pσ and pσ* orbitals stabilizes the dσ and dσ* levels to different extents, resulting in a net favorable interaction, namely [dσ*(Pt−Pt) → pσ(Pt−Pt)] (Scheme 1). This description accounts for the solution and solid-state stability as well as the photophysical properties of a wide range of stacked complexes with d^8-metal ions.[3] Another notable excited state is the MMLCT[1,4] (metal−metal-to-ligand charge-transfer) transition (Scheme 1), which occurs when two Pt(II)-diimine moieties are in close enough proximity to allow Pt(II)···Pt(II) and/or $\pi\cdots\pi$ interactions to take place, namely dσ*(Pt−Pt) → π*(diimine). In the previous work, the solid-state emissions of some stacking Pt(II)-diimine solids[1,4] and excimeric emissions of cyclometalated Pt(II) complexes[5a,b] and [Pt(diimine)$(CN)_2$][5c,d] in solution were suggested to come from an MMLCT excited state. Taking advantage of the stacking interactions, the "luminescent switch" study pioneered by Mann and co-workers[6] for the detection of volatile organic compounds (VOCs) shows that phenomena of vapochromic Pt(II) and Pd(II) complexes hold a great potential for analytical applications.

Another interesting excited state, namely an LLCT (ligand-to-ligand charge-transfer) excited state, had previously been reported in some Zn(II)[7] and Pt(II)[8] complexes containing both N-heterocyclic (diimine) and aromatic thiolate (dithiolate) ligands. Crosby and co-workers[7] introduced this concept to rationalize the visible absorption and low-energy emission spectra of some zinc(II) thiolates containing 1, 10-phenanthroline ligand. In our previous work,[9] the crystal structures and spectroscopic properties of a series of mononuclear and dinuclear Pt(II) complexes containing terminal or bridging thiolates are presented. The shift in absorption energy with changes in the electronic properties of the substituents on the diimine and thiolate ligands supports the assignment of an LLCT excited state.

Kato and co-workers[10] were able to isolate and structurally characterize two dinuclear Pt(II)-thiolate diimine isomers, *anti*- and *syn*-[Pt(bpy)(NS)]$_2$(PF_6)$_2$ (bpy = 2,2′-bipyridine, HNS = pyridine-2-thiol), and the *syn* isomer also exhibits a dramatic change in its luminescence in the presence/absence of organic vapors such as acetonitrile or ethanol. To clarify the luminescence origin of such a remarkable vapor-induced change, the authors found that the solvated *syn* isomer (dark-red form with an emission at 766 nm) shows an intermolecular Pt(II)···Pt(II) contact of 3.384(1) Å, which is short enough to suggest an intermolecular Pt(II)···Pt(II) interaction to occur between the stacked dimeric complexes. The desolvated *syn* isomer turned light-red with an emission at 644 nm, and this distinction is presumably ascribed to the absence of an intermolecular Pt(II)···Pt(II) interaction. To further investigate the interesting structural isomerism[11] of dinuclear Pt(II)-thiolate diimines and the correlation between the luminescence and intermolecular Pt(II)···Pt(II) interactions, we initiate a study on the structural and luminescent properties of dinuclear Pt(II) complexes containing 4,4′-di-*tert*-butyl-2,2′-bipyridine (d-*t*-bpy) and 2-mercaptobenzothiazol (HNS_2), 2-mercaptobenzimidazole (HN_2S), and 2-mercaptobenzoxazole (HNOS).

*To whom correspondence should be addressed.

 Published on Web 11/04/2009

Scheme 1

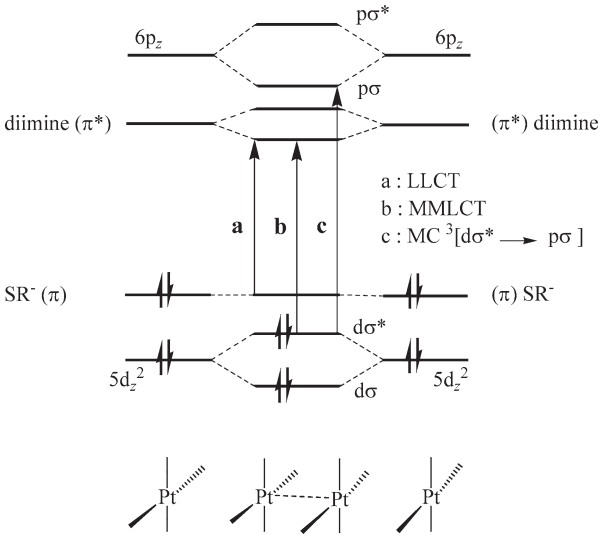

For the structural interest, *syn*-[Pt(d-*t*-bpy)(NS)]$_2$(ClO$_4$)$_2$ (HNS = pyridine-2-thiol) was also synthesized and characterized by X-ray diffraction to examine the synthetic scheme presented.

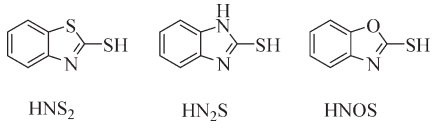

HNS$_2$ HN$_2$S HNOS

Experimental Section

General Information. 4,4′-Di-*tert*-butyl-2,2′-bipyridine (d-*t*-bpy), 2-mercaptobenzothiazole (HNS$_2$), 2-mercaptobenzimidazole (HN$_2$S), 2-mercaptobenzoxazole (HNOS), and pyridine-2-thiol (HNS) were purchased from Aldrich Chemicals. All solvents (Analytical grade) for synthesis were used without further purification, and all operations were carried out under an atmosphere of purified nitrogen. Solvents for photophysical studies were purified by literature methods. **Caution**! *Perchlorate salts are potentially explosive and should be handled with care and in small amounts*. Pt(d-*t*-bpy)Cl$_2$ was prepared by the literature method.[12]

Synthesis of *anti*-[Pt(d-*t*-bpy)(NS$_2$)]$_2$(ClO$_4$)$_2$ (1a). A clear orange solution was obtained by refluxing equimolar amounts of Pt(d-*t*-bpy)Cl$_2$ (0.3 mmol, 160 mg) and NaNS$_2$ [0.3 mmol, 57 mg; obtained from HNS$_2$ (0.3 mmol, 50 mg) and NaOMe (0.35 mmol, 19 mg) in MeOH] in MeOH (25 mL) for 4 h. Upon the addition of LiClO$_4$, a yellow solid was obtained and was recrystallized by the diffusion of Et$_2$O into a CH$_3$CN solution with a 45% yield. ^{1}H NMR (400 MHz, d_6-DMSO, 25 °C): δ (ppm) 8.69 (d, J = 6.2 Hz, Ph), 8.53 (d, J = 8.1 Hz, py), 8.49 (s, Ph), 8.39 (s, py), 8.00 (d, J = 7.9 Hz, py), 7.77 (d, J = 6.0 Hz, Ph), 7.72 (d, J = 6.2 Hz, Ph), 7.59 (t, J = 7.4 Hz, Ph), 7.53 (t, J = 7.5 Hz, Ph), 7.27 (d, J = 6.2 Hz, Ph), and 1.37 (d, J = 13.2 Hz, −CH$_3$). FT-IR: ν_{C-H} = 2961 cm^{-1}, $\nu_{C=N}$ = 1618 cm^{-1}, and ν_{Cl-O} = 1091 cm^{-1}. ESI-MS: [M-2ClO$_4$]$^{2+}$, m/e = 629.8 (22%). Anal. Calcd (%) for C$_{50}$H$_{56}$Cl$_2$N$_6$O$_8$Pt$_2$S$_4$: C, 41.14; H, 3.84; N, 5.76. Found (%): C, 40.89; H, 3.78; N, 5.97.

Synthesis of *syn*-[Pt(d-*t*-bpy)(NS$_2$)]$_2$(ClO$_4$)$_2$ (1b). The above filtrate was reduced to dryness, and then the residue was dissolved in CH$_2$Cl$_2$. Addition of hexane to the CH$_2$Cl$_2$ solution gave rise to an orange solid, which was recrystallized by diffusion of Et$_2$O into a MeOH solution with a 30% yield. ^{1}H NMR (400 MHz, d_6-DMSO, 25 °C): δ (ppm) 8.90 (d, J = 6.2 Hz, py), 8.42 (s, py), 8.01 (d, J = 6.3 Hz, py), 7.67 (d, J = 6.2 Hz, Ph), 7.58 (dd, J = 6.2, 2.0 Hz, Ph), 7.40 (m, Ph), 7.26 (t, J = 4.2 Hz, Ph), and 1.36 (d, J = 12.7 Hz, −CH$_3$). FT-IR: ν_{C-H} = 2963 cm^{-1}, $\nu_{C=N}$ = 1617 cm^{-1}, and ν_{Cl-O} = 1088 cm^{-1}. ESI-MS: [M − 2ClO$_4$]$^{2+}$, m/e = 629.0 (23.0%). Anal. Calcd (%) for C$_{50}$H$_{56}$Cl$_2$N$_6$O$_8$Pt$_2$S$_4$: C, 41.14; H, 3.84; N, 5.76. Found (%): C, 41.39; H, 4.09; N, 5.97.

Synthesis of *anti*-[Pt(d-*t*-bpy)(N$_2$S)]$_2$(PF$_6$)$_2$ (2a). The synthesis is similar to that of **1a**, except EtOH and PF$_6^-$ were used instead of MeOH and ClO$_4^-$, respectively. The yellow precipitate was recrystallized by the diffusion of Et$_2$O into a MeOH/CHCl$_3$ solution with a 35% yield. ^{1}H NMR (400 MHz, d_6-DMSO, 25 °C): 8.81 (d, J = 6.1 Hz, py), 8.46 (s, Ph), 8.38 (s, py), 7.75 (m, Ph), 7.27 (m, py), and 1.39 (d, J = 21.0 Hz, −CH$_3$). FT-IR: ν_{C-H} = 2963 cm^{-1}, $\nu_{C=N}$ = 1619 cm^{-1}, and ν_{P-F} = 828 cm^{-1}. ESI-MS: [M − 2PF$_6$]$^{2+}$, m/e = 612.3 (100.0%). Anal. Calcd (%) for C$_{50}$H$_{58}$F$_{12}$N$_8$P$_2$Pt$_2$S$_2$: C, 39.63; H, 3.86; N, 7.39. Found (%): C, 39.92; H, 3.78; N, 7.28.

Synthesis of *syn*-[Pt(d-*t*-bpy)(N$_2$S)]$_2$(ClO$_4$)$_2$ (2b). The synthesis is similar to that of **1b**, except EtOH was used instead of MeOH. The orange filtrate stood in air for a couple of days to give crystalline compounds with a 52% yield. ^{1}H NMR (400 MHz, d_6-DMSO, 25 °C): 13.6 (s, im), 8.80 (d, J = 6.4 Hz, py), 8.47 (s, py), 8.38 (s, ph), 7.75 (dd, J = 6.2, 20.0 Hz, ph), 7.27 (m, py), and 1.37 (d, J = 20.4 Hz, −CH$_3$). FT-IR: ν_{C-H} = 2967 cm^{-1}, $\nu_{C=N}$ = 1620 cm^{-1}, and ν_{Cl-O} = 1114 cm^{-1}. ESI-MS: [M − 2ClO$_4$]$^{2+}$, m/e = 612.3 (100.0%). Anal. Calcd (%) for C$_{50}$H$_{58}$Cl$_2$N$_8$O$_8$Pt$_2$S$_2$: C, 42.17; H, 4.10; N, 7.87. Found (%): C, 42.39; H, 4.27; N, 7.79.

Synthesis of *syn*-[Pt(d-*t*-bpy)(NOS)]$_2$(ClO$_4$)$_2$ (3). The synthesis is similar to that of **2b**. The orange filtrate was stood in air for a couple of days to give crystalline solids with a 37% yield. However, both methods can only isolate the *syn* isomer, and the isolation of the *anti* isomer was unsuccessful. ^{1}H NMR (400 MHz, d_6-DMSO, 25 °C): 9.17 (d, J = 6.2 Hz, py), 8.49 (s, py), 8.42 (s, py), 8.03 (d, J = 6.2 Hz, Ph), 7.76 (dd, J = 21.0, 7.8 Hz, Ph), 7.57 (d, J = 6.2 Hz, Ph), 7.35 (dt, J = 21.3, 8.0 Hz, Ph), 7.22 (d, J = 6.1 Hz, py), and 1.36 (d, J = 12.7 Hz, −CH$_3$). FT-IR: ν_{C-H} = 2964 cm^{-1}, $\nu_{C=N}$ = 1619 cm^{-1}, and ν_{Cl-O} = 1091 cm^{-1}. ESI-MS: [M − 2ClO$_4$]$^{2+}$, m/e = 613.3 (100.0%). Anal. Calcd (%) for C$_{50}$H$_{56}$Cl$_2$N$_6$O$_{10}$Pt$_2$S$_2$: C, 42.11; H, 3.96; N, 5.89. Found (%): C, 42.35; H, 4.04; N, 5.61.

Synthesis of *syn*-[Pt(d-*t*-bpy)(NS)]$_2$(ClO$_4$)$_2$ (4b). The synthesis is similar to that of **2b**. The red-orange filtrate was stood in air for a couple of days to give crystalline compounds with a 48% yield. ^{1}H NMR (400 MHz, d_6-DMSO, 25 °C): δ (ppm) 8.63 (d, J = 6.2 Hz, py), 8.47 (s, py), 7.74 (d, J = 6.2 Hz, Ph), 7.63 (d, J = 8.0 Hz, Ph), 7.26 (d, J = 4.7 Hz, Ph), 7.22 (q, J = 1.8 Hz, Py), and 1.36 (d, J = 12.7 Hz, −CH$_3$). FT-IR: ν_{C-H} = 2961 cm^{-1}, $\nu_{C=N}$ = 1619 cm^{-1}, and ν_{Cl-O} = 1089 cm^{-1}. ESI-MS: [M − 2ClO$_4$]$^{2+}$, m/e = 573.3 (100.0%). Anal. Calcd (%) for C$_{46}$H$_{56}$Cl$_2$N$_6$O$_{10}$Pt$_2$S$_2$: C, 40.09; H, 4.10; N, 6.10. Found (%): C, 39.87; H, 4.03; N, 5.88.

Physical Measurements and Instrumentation. NMR: Bruker DPX 400 MHz NMR; deuterated solvents with the usual standards. Infrared spectra (IR) were recorded from KBr pellets on a Perkin-Elmer PC 16 FTIR spectrometer. UV/vis spectra were recorded on a Cary 3E instrument from Ocean Optics, and HP and steady state emission spectra were recorded on a Hitachi F-7000 spectrophotometer.

X-ray Crystallography. Suitable single crystals were each mounted on a glass capillary, and data collection was carried out on a Bruker SMART CCD diffractometer with Mo radiation (0.71073 Å). A preliminary orientation matrix and unit cell parameters were determined from 3 runs of 15 frames each, with each frame corresponding to a 0.3° scan in 20 s, followed by spot integration and least-squares refinement. Data were measured using an ω scan of 0.3° per frame for 20 s until a complete hemisphere had been collected. Cell parameters were retrieved using SMART software and refined with SAINT on all observed reflections. Data reduction was performed with the SAINT software and corrected for Lorentz and polarization effects. Absorption corrections were applied with the program SADABS. The structure was solved by direct methods with the SHELXS-97[13d] program and refined by full-matrix least-squares methods on F^2 with SHELXL-97 All non-hydrogen atomic positions were located in difference Fourier maps and refined anisotropically. Hydrogen atoms were constrained to the ideal geometry using an appropriate riding model. Detailed data collection and refinement are summarized in Table 1, and selected bond distances and angles are summarized in Table 2.

Table 1. Crystallographic Data of 1a, 1b, 2a, 2b, 3, and 4b

	1a	**1b**·CH_3OH	**2a**·$0.5CH_3OH$·$2C_4H_{10}O$	**2b**·C_2H_5OH	**3**·CH_3OH	**4b**·$2H_2O$
empirical formula	$C_{50}H_{56}Cl_2N_6O_8Pt_2S_4$	$C_{51}H_{60}Cl_2N_6O_9Pt_2S_4$	$C_{58.5}H_{78}F_{12}N_8O_{2.5}P_2Pt_2S_2$	$C_{52}H_{63}Cl_2N_8O_9Pt_2S_2$	$C_{51}H_{60}Cl_2N_6O_{11}Pt_2S_2$	$C_{47}H_{56}Cl_2N_6O_{10}Pt_2S_2$
formula weight	1458.33	1490.37	1677.53	1469.30	1458.25	1390.18
crystal system	tetragonal	triclinic	monoclinic	triclinic	triclinic	monoclinic
space group (no.)	$I4_1/a$	$P\bar{1}$	$P2_1/c$	$P\bar{1}$	$P\bar{1}$	$P2_1/c$
a (Å)	12.0789(7)	12.6956(2)	16.7779(2)	11.7638(10)	11.6084(5)	14.0251(11)
b (Å)	12.0789(7)	15.4076(2)	24.0069(2)	14.6474(13)	14.2276(7)	12.3473(10)
c (Å)	76.793(6)	16.6151(2)	19.1498(2)	17.9254(16)	18.0294(8)	34.0632(19)
α (deg)	90	66.3302(9)	90	68.308(2)	68.226(1)	90
β (deg)	90	80.2927(8)	115.2853(5)	82.091(2)	82.602(1)	113.738(3)
γ (deg)	90	79.9283(8)	90	87.821(2)	88.334(1)	90
V (Å^3), Z	11204.1(13), 8	2913.3(1), 2	6974.27(12), 4	2842.4(4), 2	2741.7(2), 2	5399.7(7), 4
F(000) (e)	5728	1468	3324	1450	1436	2728
μ (Mo Kα) (mm^{-1})	5.289	5.088	4.190	5.144	5.334	5.410
T (K)	295(2)	295(2)	150(2)	294(2)	150(2)	293(2)
reflections collected	49859	42868	41665	28518	36564	53900
independent reflections ($F_o \geq 2\sigma(F_o)$)	6854 (R_{int} = 0.101)	13386 (R_{int} = 0.066)	15929 (R_{int} = 0.044)	10385 (R_{int} = 0.066)	12596 (R_{int} = 0.053)	9878 (R_{int} = 0.145)
refined parameters	343	681	771	708	681	679
goodness-of-fit on F^2	1.131	1.015	1.022	1.008	1.101	1.162
R^a, $R_w{}^b$ ($I \geq 2\sigma(I)$)	0.080, 0.157	0.047, 0.092	0.053, 0.143	0.052, 0.102	0.045, 0.093	0.096, 0.180
R^a, $R_w{}^b$ (all data)	0.142, 0.183	0.091, 0.109	0.081, 0.160	0.099, 0.128	0.065, 0.101	0.141, 0.201

$^a R = \sum||F_o| - |F_c||/\sum|F_o|$. $^b wR_2 = \{\sum w(F_o^2 - F_c^2)^2/\sum[w(F_o^2)^2]\}^{1/2}$.

Theoretical Method. The density functional B3LYP[14a,b]/LanL2DZ[14c] level of calculations was carried out for the dimers of *syn*-$[Pt(d\text{-}t\text{-}bpy)(NS_2)]_2^{2+}$, *syn*-$[Pt(d\text{-}t\text{-}bpy)(N_2S)]_2^{2+}$, *syn*-$[Pt(d\text{-}t\text{-}bpy)(NOS)]_2^{2+}$, and *syn*-$[Pt(bpy)(NS)]_2^{2+}$[10] in the corresponding crystal geometries. The Gaussian03 program[15] was utilized in the electronic structure calculations.

Results and Discussion

To investigate this interesting structural isomerism of a series of *anti* and *syn* isomers of dinuclear Pt(II)-thiolate diimines, an efficient method has been developed in this laboratory, and the synthetic scheme for **1a** and **1b** is shown in Scheme 2 as a representative example. In a one-pot reaction, the *anti* isomer can be first isolated from the precipitate upon addition of $LiClO_4$ or NH_4PF_6 to the solution and the *syn* isomer can be later obtained from the filtrate by a layer method (CH_2Cl_2/hexane). The isolated complexes are air stable and emissive in the solid state but nonemissive in solution.

Description of Crystal Structures. The molecular structures of complexes **1a** and **1b** are shown in parts a and b, respectively, of Figure 1, as representative examples. Because of the high structural similarity of the complexes studied, we only choose **1a** and **1b** for the detailed structural description. **1a** (*anti* isomer) and **1b** (*syn* isomer) crystallized in the $I4_1/a$ and $P\bar{1}$ space groups, respectively, and each Pt(II) center adopts a square-planar geometry. The Pt(II) center coordinates to three nitrogen atoms and one sulfur atom in **1a**, but it coordinates to two nitrogen atoms and two sulfur atoms for one Pt(II) center and four nitrogen atoms for the other Pt(II) center in **1b**. In this regard, the *anti* isomer has a head-to-tail configuration of two μ_2-bridging NS_2 groups with a 2-fold axis passing through the midpoint of the Pt(II)···Pt(II) axis, whereas the *syn* isomer has a head-to-head configuration of two μ_2-bridging NS_2 groups constituting a different coordination environment of the Pt(II) centers with respect to that of **1a**. The intramolecular Pt(II)···Pt(II) distances of **1a** and **1b** are 2.9727(9) and 2.9730(4) Å, respectively, which are comparable to those of

Scheme 2

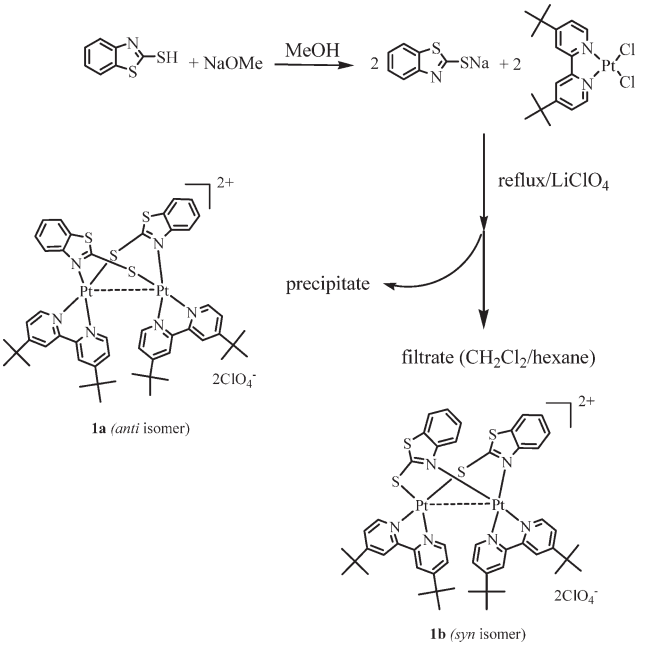

syn-$[Pt(bpy)(NS)]_2(PF_6)_2$ [2.923(1) Å],[10] *anti*-$[Pt(bpy)(NS)]_2(PF_6)_2$ [2.997(1) Å],[10] and *anti*-$[Pt(d\text{-}t\text{-}bpy)(NS)]_2(ClO_4)_2$ [2.917(2) Å][9] but slightly shorter than those of *syn*-$[Pt(en)(C_5H_4NS)]_2Cl_2$ [en = ethylenediamine, 3.083(1) Å][16] and *syn*-$[Pt(en)(4\text{-}MeC_5H_3NS)]_2Cl_2$ [3.101(1) Å].[16] They are, however, comparable to the value of 2.925(1) Å in $K_4[Pt_2(P_2O_5H_2)_4]$.[17] Indeed, these short intramolecular distances would most likely lead to weak intramolecular Pt(II)···Pt(II) and/or $\pi\cdots\pi$ interactions in the solid state.

The Pt−S distance is 2.296(3) Å, and the Pt−N (NS_2) and Pt−N_{ave} (d-*t*-bpy) distances are 2.010(8) and 2.025(8) Å, respectively, for **1a**; the average Pt−S distance is 2.290(2) Å, and the Pt−N_{ave} (NS_2) and Pt−N_{ave} (d-*t*-bpy) distances are 2.030(5) and 2.028(6) Å, respectively, for **1b**. The average

Table 2. Selected Bond Distances (Å) and Angles (deg) of 1a, 1b, 2a, 2b, 3, and 4b

1a	Pt(1)−N(1)	2.037(8)	Pt(1)−N(2)	2.012(7)
	Pt(1)−N(3)	2.010(8)	Pt(1)−S(1)	2.296(3)
	S(1)−C(19)	1.730(12)	S(2)−C(25)	1.728(14)
	N(2)−Pt(1)−N(1)	80.0(3)	N(2)−Pt(1)−S(1)	96.2(2)
	N(1)−Pt(1)−S(1)	172.8(2)		
1b	Pt(1)−N(3)	2.047(6)	Pt(1)−N(4)	2.059(5)
	Pt(2)−N(1)	2.032(5)	Pt(2)−N(2)	2.028(5)
	Pt(2)−N(5)	2.006(4)	Pt(2)−N(6)	1.998(5)
	Pt(1)−S(1)	2.294(2)	Pt(1)−S(3)	2.286(2)
	S(1)−C(1)	1.719(7)	S(3)−C(8)	1.717(8)
	N(3)−Pt(1)−N(4)	79.4(2)	N(6)−Pt(2)−N(5)	80.4(2)
	N(6)−Pt(2)−N(2)	96.8(2)	N(5)−Pt(2)−N(2)	175.9(2)
	N(6)−Pt(2)−N(1)	176.9(2)	N(5)−Pt(2)−N(1)	96.9(2)
	N(2)−Pt(2)−N(1)	86.0(2)	N(3)−Pt(1)−S(3)	175.1(2)
	N(4)−Pt(1)−S(3)	96.0(2)	N(3)−Pt(1)−S(1)	96.0(2)
	N(4)−Pt(1)−S(1)	173.2(2)	S(3)−Pt(1)−S(1)	88.5(1)
2a	Pt(1)−N(5)	2.018(6)	Pt(1)−N(1)	2.022(7)
	Pt(1)−N(6)	2.045(6)	Pt(2)−N(3)	2.005(6)
	Pt(2)−N(7)	2.019(6)	Pt(2)−N(8)	2.037(6)
	Pt(1)−S(2)	2.289(2)	Pt(2)−S(1)	2.296(2)
	S(1)−C(1)	1.716(8)	S(2)−C(8)	1.729(8)
	N(5)−Pt(1)−N(1)	175.9(2)	N(5)−Pt(1)−N(6)	79.9(3)
	N(1)−Pt(1)−N(6)	96.0(3)	N(3)−Pt(2)−N(7)	175.4(2)
	N(3)−Pt(2)−N(8)	95.7(3)	N(7)−Pt(2)−N(8)	79.8(3)
	N(5)−Pt(1)−S(2)	96.3(2)	N(1)−Pt(1)−S(2)	87.7(2)
	N(6)−Pt(1)−S(2)	174.3(2)	N(3)−Pt(2)−S(1)	87.4(2)
	N(7)−Pt(2)−S(1)	97.2(2)	N(8)−Pt(2)−S(1)	174.6(2)
2b	Pt(1)−N(1)	2.042(8)	Pt(1)−N(2)	2.043(8)
	Pt(2)−N(3)	2.005(7)	Pt(2)−N(4)	2.019(8)
	Pt(2)−N(7)	2.022(4)	Pt(2)−N(6)	2.032(4)
	Pt(1)−S(1)	2.301(3)	Pt(1)−S(2)	2.303(3)
	S(1)−C(37)	1.723(11)	S(2)−C(44)	1.709(11)
	N(1)−Pt(1)−N(2)	79.9(3)	N(3)−Pt(2)−N(4)	79.6(3)
	N(3)−Pt(2)−N(7)	175.4(2)	N(4)−Pt(2)−N(7)	95.8(3)
	N(3)−Pt(2)−N(6)	98.8(2)	N(4)−Pt(2)−N(6)	175.1(3)
	N(7)−Pt(2)−N(6)	85.8(1)	N(1)−Pt(1)−S(1)	95.2(3)
	N(2)−Pt(1)−S(1)	174.6(2)	N(1)−Pt(1)−S(2)	172.7(2)
	N(2)−Pt(1)−S(2)	96.1(2)	S(1)−Pt(1)−S(2)	89.1(1)
3	Pt(1)−N(3)	1.996(5)	Pt(1)−N(4)	2.003(5)
	Pt(1)−N(2)	2.014(5)	Pt(1)−N(1)	2.016(5)
	Pt(2)−N(6)	2.037(5)	Pt(2)−N(5)	2.047(5)
	Pt(2)−S(2)	2.297(2)	Pt(2)−S(1)	2.302(2)
	S(1)−C(1)	1.705(7)	S(2)−C(8)	1.686(7)
	N(3)−Pt(1)−N(4)	80.0(2)	N(3)−Pt(1)−N(2)	95.1(2)
	N(4)−Pt(1)−N(2)	175.1(2)	N(3)−Pt(1)−N(1)	174.7(2)
	N(4)−Pt(1)−N(1)	98.2(2)	N(2)−Pt(1)−N(1)	86.6(2)
	N(6)−Pt(2)−N(5)	79.4(2)	N(6)−Pt(2)−S(2)	171.8(2)
	N(5)−Pt(2)−S(2)	96.3(2)	N(6)−Pt(2)−S(1)	95.4(2)
	N(5)−Pt(2)−S(1)	174.3(2)	S(2)−Pt(2)−S(1)	89.1(1)
4b	Pt(1)−N(2)	1.993(13)	Pt(1)−N(5)	2.010(13)
	Pt(1)−N(1)	2.017(11)	Pt(1)−N(6)	2.022(12)
	Pt(2)−N(3)	2.032(12)	Pt(2)−N(4)	2.051(14)
	Pt(2)−S(1)	2.274(5)	Pt(2)−S(2)	2.276(5)
	S(1)−C(37)	1.752(19)	S(2)−C(42)	1.759(18)
	N(2)−Pt(1)−N(5)	174.6(5)	N(2)−Pt(1)−N(1)	81.2(5)
	N(5)−Pt(1)−N(1)	94.4(5)	N(2)−Pt(1)−N(6)	96.7(5)
	N(5)−Pt(1)−N(6)	87.3(5)	N(1)−Pt(1)−N(6)	172.2(5)
	N(3)−Pt(2)−N(4)	78.4(6)	N(3)−Pt(2)−S(1)	95.9(4)
	N(4)−Pt(2)−S(1)	172.6(5)	N(3)−Pt(2)−S(2)	175.1(4)
	N(4)−Pt(2)−S(2)	96.8(4)	S(1)−Pt(2)−S(2)	89.0(2)

Pt−S distance of 2.290(2)−2.296(3) Å appears to correspond more closely to Pt(II)−thiolate than to Pt(II)−thione distances. Indeed, typical Pt(II)−thiolate distances occur in the range of 2.281−2.333 Å, whereas the Pt(II)−thione distances lie between 2.339 and 2.362 Å.[18] On the basis of the observed bonding parameters, the μ_2-bridging NS_2 is inferred to be in the thiolate form, rather than in the thione form. The mean values of C−S distances are 1.729(14) and 1.718(8) Å for **1a** and **1b**, respectively. Indeed, the bond parameters of **2a**, **2b**, and **3** are quite similar to those of **1a** and **1b**.

It is noted that the *syn* isomers of dinuclear Pt(II)-thiolate diimines (**1b**, **2b**, and **3**) all show intermolecular Pt(II)···Pt(II)

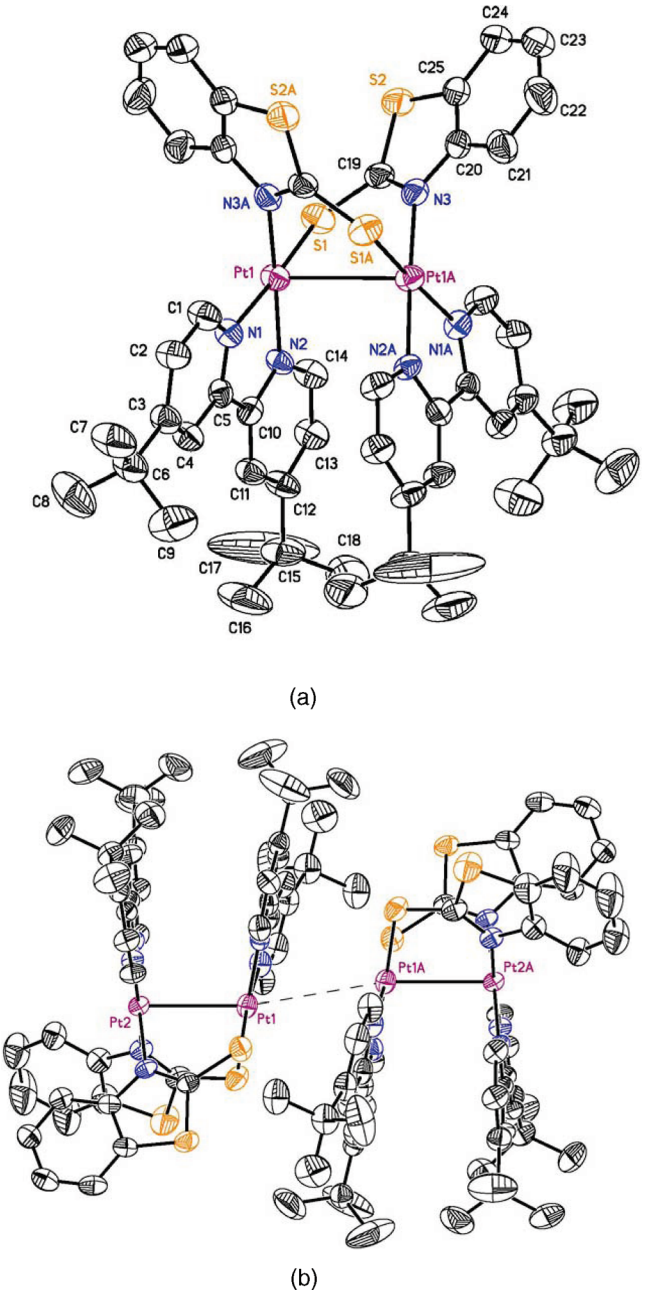

Figure 1. (a) Perspective view of **1a** and (b) dimeric structure of **1b** found in the crystal lattice, showing a long intermolecular Pt(II)···Pt(II) contact of 3.859 Å.

contacts of 3.510(4)−3.859(4) Å (**1b**, 3.859(4) Å; **2b**, 3.579(6) Å; **3**, 3.510(4) Å); some crystals are cracked upon cooling to the low temperature, and thus, it made the temperature-dependence X-ray diffraction studies impossible. In fact, the distance of 3.859(4) Å falls beyond the range of 3.0−3.5 Å for the linear-chain solids of Pt(II)-diimine complexes,[1] which are generally considered as the presence of weak Pt(II)···Pt(II) interactions, but the values of 3.579(6) and 3.510(4) Å are only slightly longer than those of linear-chain solids, *syn*-$[Pt(bpy)(NS)]_2(PF_6)_2$ [3.384(1) Å],[15] $[Pt(terpy)Cl](CF_3SO_3)$ [3.329(1) Å],[4a] and the red form of $Pt(bpy)Cl_2$ [3.450 Å].[19] Thus, the presence of weak Pt(II)···Pt(II) interactions for the latter is also possible. Intriguingly, the occupied molecular orbitals (MO) obtained by the B3LYP/LanL2DZ calculations clearly show there are bonding interactions between intermolecular Pt(II) centers for *syn*-$[Pt(bpy)(NS)]_2(PF_6)_2$, **2b**, **3**, and even **1b**, whose

intermolecular Pt(II)···Pt(II) distance is 3.859(4) Å. In addition, the *syn* isomers also show weak intermolecular $\pi\cdots\pi$ contacts between the neighboring phenyl pairs (centroid to centoid distances and angles between the centroid → centroid vector and any normal to phenyl rings: 3.72 Å and 19.69° for **1b**, 3.76 Å and 22.72° for **2b**, 3.78 Å and 24.58° for **3**). According to Janiak's report,[20] the $\pi\cdots\pi$ interaction is defined as when the above distances and angles are less than 3.80 Å and 20.00°, respectively. Thus, the $\pi\cdots\pi$ interaction strength for the *syn* isomers obeys the following order: **1b** > **2b** > **3**. However, the *anti* ones (**1a** and **2a**) have no short intermolecular Pt(II)···Pt(II) (i.e., 7.69 Å for **1a** and 9.26 Å for **2a**) and $\pi\cdots\pi$ contacts, and this is most likely ascribed to the steric hindrance provided by two thiolates in an *anti* conformation.

For structural interest, **4b** was synthesized and characterized by X-ray diffraction, as shown in the structural information. The bond parameters are similar to those of its *anti* counterpart (**4a**), where it has been reported in our previous study.[9] Unlike **4a**, the intermolecular Pt(II)···Pt(II) (3.978(1) Å) and $\pi\cdots\pi$ contacts (centroid to centoid distances and angles between the centroid → centroid vector and any normal to phenyl rings: 3.99 Å and 33.29°) for **4b** can be found, but they are in fact too long to be thought of as any weak interaction. Most significantly, we have proved our synthetic scheme is a successful strategy toward the isolation of interesting structural isomers of dinuclear Pt(II)-thiolate diimines. In addition, the dihedral and torsional angles for two d-*t*-bpy ligands in dinuclear Pt(II)-thiolate diimines have been calculated to be 23.3 and 24.0° for **1a**, 17.8 and 25.1° for **1b**, 21.8 and 24.5° for **2a**, 18.8 and 24.6° for **2b**, 17.9 and 25.3° for **3**, and 19.1 and 24.7° for **4b**, respectively. Thus, both angles fall in a similar range.

Emission Spectra. As mentioned in the previous section, the red form of $Pt(bpy)Cl_2$ contains a weak Pt(II)···Pt(II) interaction of 3.450 Å,[19] and it was suggested that such a weak interaction is closely related to its emission energy. Miskowski et al. studied the low temperature emission of the complex.[1b] Their results showed that the red-shift of 930 cm^{-1} in the emission energy was observed upon cooling the solid samples, and the excited state was therefore assigned to MMLCT. This assignment is used to rationalize recent results based on pyrazolate-bridged and cyclometalated Pt(II) complexes with intramolecular Pt(II)···Pt(II) interactions of 2.8343(6)−3.3763(7) Å by Thompson and co-workers.[1d]

To examine the correlation between the luminescence and intermolecular Pt(II)···Pt(II) interactions for dinuclear Pt(II)-thiolate diimines, we set out to measure the solid-state luminescence at room temperature and at 77 K for **1a**, **1b**, **2a**, **2b**, and **3**, and the emission spectra of **1a** and **1b** are shown in parts a and b, respectively, of Figure 2 as representative examples. Upon photoexcitation at 300−350 nm, both **1a** and **1b** show low-energy emissions with a maximum at *ca.* 548 and 588 nm at room temperature, respectively. Upon cooling these solid samples to 77 K, both **1a** and **1b** show red-shifts of 550 cm^{-1} (from 548 to 565 nm) and of 1260 cm^{-1} (from 588 to 635 nm) in emission energies, respectively, and there is an additional weak emission at *ca.* 553 nm for **1b**. For the other complexes (**2a, 2b**, and **3**), their emission spectra at room temperature are quite similar (562−573 nm), but their low-temperature emission spectra differ to some extent (572−602 nm). The red-shifts in emission energies caused by the temperature decrease are within 190−840 cm^{-1} for **2a**, **2b**, and **3**, and these data and those of **1a** and **1b** are summarized in Table 3. Notably, the cooling effect led to red-shifts of 310−550 cm^{-1} for the *anti* isomers (**1a** and **2a**) and 190−1260 cm^{-1} for the *syn* isomers (**1b**, **2b**, and **3**), respectively. Thus, there is no obvious correlation between emission energies and intermolecular Pt(II)···Pt(II) interactions. This can also be evidenced by the fact that **1b**, having the largest red-shift, contains the longest intermolecular Pt(II)···Pt(II) contact (3.859(4) Å) and **3**, having the smallest red-shift, contains the shortest intermolecular Pt(II)···Pt(II) contact (3.510(4) Å) for the *syn* isomers. Indeed, the solvated form of *syn*-$[Pt(bpy)(NS)]_2(ClO_4)_2$ was proved to have an intermolecular Pt(II)···Pt(II) interaction of 3.384(1) Å, but the desolvated form is so far unknown for its crystal structure. Although the spectroscopic data can definitely confirm the presence of Pt(II)···Pt(II) interactions for the Pt(II) diimines and/or pyrazolates,[1] it still remains uncertain for Pt(II) thiolates.[9] This is because the Pt(II) diimines and/or pyrazolates have well-known MMLCT excited states. However, the Pt(II) thiolates were previously known to have an LLCT excited state,[8,9] and their Pt(II)···Pt(II) interactions are not primarily responsible for the emissions.[9] In Eisenberg's previous work,[8c−h] the metal/thiolate-to-diimine charge-transfer transitions (M/LLCT) are suggested to rationalize the excited states in a series of mononuclear Pt(II) thiolates.[8c−h] In fact, no intermolecular Pt(II)···Pt(II) interaction can be observed in the solid states. In this regard, we reason that the presence of significant Pt(II)···Pt(II) interactions involved in the excited state is still possible. Since Kato's solvated *syn*-$[Pt(bpy)(NS)]_2(ClO_4)_2$ has a short Pt(II)···Pt(II) contact ($Pt(II)\cdots Pt(II)_{inter}$ = 3.384(1) Å), the MMLCT excited state instead of LLCT may be tentatively assigned.

The HOMOs and LUMOs of **1b**, **2b**, **3**, and *syn*-$[Pt(bpy)(NS)]_2(PF_6)_2$ (Supporting Information) indicate that all four

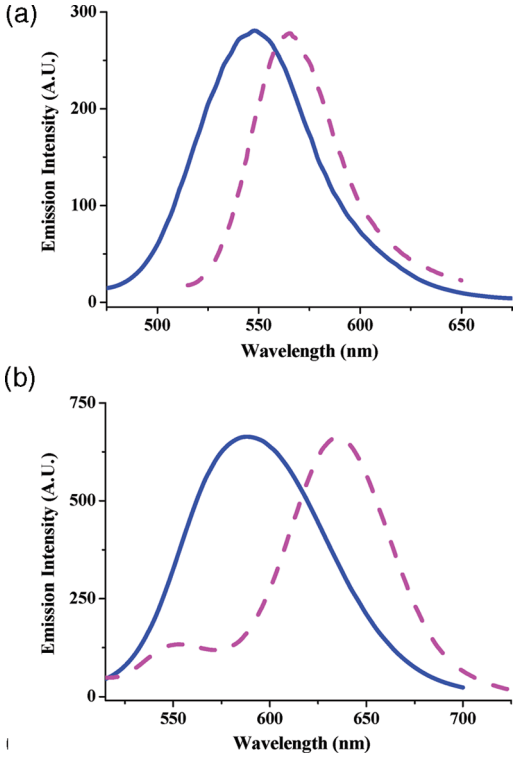

Figure 2. Solid-state emission spectra of (a) **1a** and (b) **1b** at room temperature (blue solid line) and at 77 K (pink dashed line).

Table 3. Pt···Pt$_{intra}$ and Pt···Pt$_{inter}$/π···π_{inter} Distances of Dinuclear Pt(II)−Thiolate Diimines and Their Solid-State Emission at Room Temperature and at 77 K and Glass (Ethanol/Methanol = 1:4) Emission at 77 K

complexes	Pt···Pt$_{intra}$ (Å)	Pt···Pt$_{inter}$ (Å), π···π_{inter} (Å/deg)[a]	λ_{max} at 298/77 K (red shift) glass (ethanol/methanol = 1:4) at 77 K
anti-[{Pt(d-*t*-bpy)(NS$_2$)}$_2$]$^{2+}$ (**1a**)	2.9727(9)		548/565 (550 cm^{-1}), 558
syn-[{Pt(d-*t*-bpy)(NS$_2$)}$_2$]$^{2+}$ (**1b**)	2.973(4)	3.859(4), 3.72/19.69	588/635 (1260 cm^{-1}), 567
anti-[{Pt(d-*t*-bpy)(N$_2$S)}$_2$]$^{2+}$ (**2a**)	2.9788(4)		562/572 (310 cm^{-1}), 559
syn-[{Pt(d-*t*-bpy)(N$_2$S)}$_2$]$^{2+}$ (**2b**)	3.0079(6)	3.579(6), 3.76/22.72	573/602 (840 cm^{-1}), 563
syn-[{Pt(d-*t*-bpy)(NOS)}$_2$]$^{2+}$ (**3**)	3.003(4)	3.510(4), 3.78/24.58	566/572 (190 cm^{-1}), 548

[a] Centroid to centoid distances (Å) and angles (deg) between the centroid → centroid vector and any normal to phenyl rings.

HOMOs are of Pt(II)···Pt(II) σ antibonding character and involved four Pt(II) centers, respectively, and that the four LUMOs mainly stem from ligands. If the assumption that the emission involved the HOMO and LUMO of each compound is made, it would suggest that the intermolecular Pt(II)···Pt(II) interaction in fact takes part in the solid-state luminescence of **1b**, **2b**, **3b**, and *syn*-[Pt(bpy)(NS)]$_2$(PF$_6$)$_2$. Thus, our theoretical calculations suggest that intermolecular Pt(II)···Pt(II) interactions are involved in the excited states for the above four complexes. However, the larger portions of *syn*-[Pt(bpy)(NS)]$_2$(PF$_6$)$_2$ (Pt(II)···Pt(II)$_{inter}$ = 3.384(1) Å) and smaller portions of **1b**, **2b**, and **3b** (Pt(II)···Pt(II)$_{inter}$ = 3.510(4)−3.859(4) Å) from intermolecular Pt(II) centers support our assignments of M/LLCT for the former and LLCT for the latter.

The intermolecular Pt(II)···Pt(II) interactions are not primarily responsible for the red-shifts in the solid-state luminescence upon cooling the solid samples, although our theoretical calculations suggest that intermoleculatr Pt(II)···Pt(II) interactions may be involved in the excited states. In fact, the complexes with larger red-shifts of 1260 (**1b**) and 840 cm^{-1} (**2b**) are in parallel with their decreased intermolecular π···π contacts (centroid to centoid distances of the paired rings: 3.72 Å for **1b** and 3.76 Å for **2b**), and in turn the smaller red-shifts of 190−550 cm^{-1} for **1a**, **2a** (no π···π contact), and **3** (a poor π···π contact of 3.78 Å) can also be correlated with their π···π interaction strength upon cooling the solid samples. To clarify if the intermolecular π···π interactions instead of Pt(II)···Pt(II) ones are really responsible for the luminescence, glass luminescence measurements were conducted, and those of **1a** and **1b** are shown in Figure 3a as representative examples. It was found that the glass (ethanol/methanol = 1:4) at 77 K luminesces at 558 and 567 nm for **1a** and **1b**, respectively. Since the intermolecular π···π interaction can be expected to be absent in a glass solution for **1b** at a concentration of 10^{-5} M, its emission blue-shifting to that of the solid state at 77 K can be anticipated. Indeed, a large blue-shift of 1890 cm^{-1} in the emission energy for **1b** was observed. Because there is no π···π interaction observed in the crystal lattice for **1a**, hence a small blue-shift of 220 cm^{-1} observed from solid state to glass at 77 K is not unreasonable. Although the absorptions of **1a** and **1b** can be found to follow Beer's law at concentrations of 10^{-5}−10^{-4} M (Supporting Information), the concentration-dependence glass luminescence measurements are still carried out and displayed in parts b and c, respectively, of Figure 3. Figure 3c shows the increasing emission at 567 nm is concomitant with an additional tailing at 600−700 nm for **1b** upon increasing concentrations from 10^{-5} to 10^{-4} M, but a similar phenomenon is not observed for **1a** in Figure 3b. In this regard, the concentration-dependence glass luminescence measurements further support that intermolecular π···π interactions instead of Pt(II)···Pt(II) ones are most likely correlated with the solid-state luminescence.

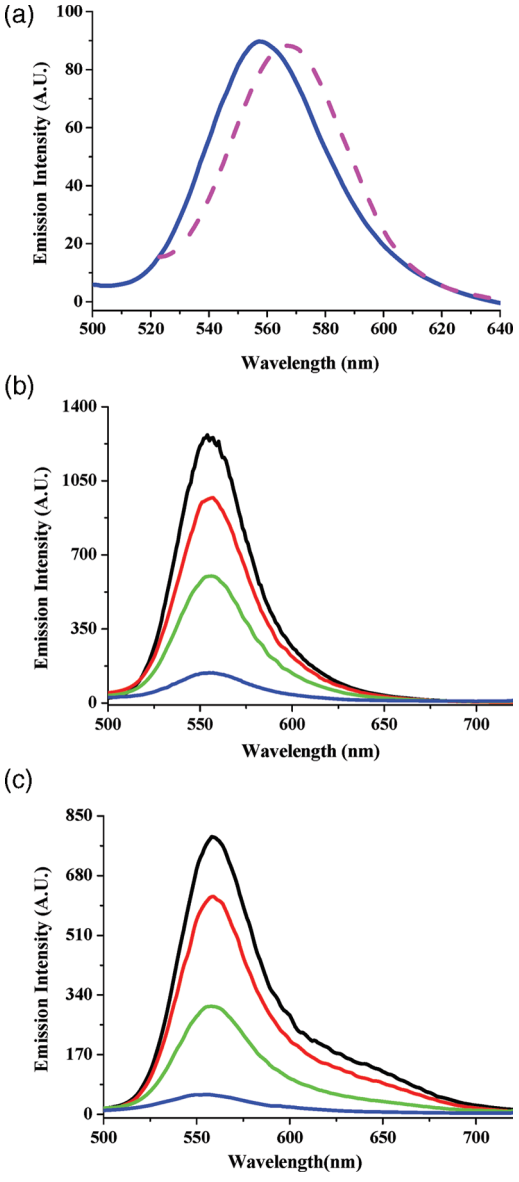

Figure 3. (a) Glass (ethanol/methanol = 1:4, 2×10^{-5} M) emission spectra of **1a** (blue solid line) and **1b** (pink dashed line) at 77 K, and the concentration-dependence emission spectra of (b) **1a** and (c) **1b** at concentrations of 10^{-5} (blue), 5×10^{-5} (green), 10^{-4} (red), and 2×10^{-4} M (black).

Conclusions

An efficient method has been developed to isolate a series of *anti* and *syn* isomers of dinuclear Pt(II)-thiolate diimines, with

an interesting phenomenon of the structural isomerism. It is noted that the *syn* isomers of dinuclear Pt(II)-thiolate diimines all show intermolecular Pt(II)···Pt(II) contacts of 3.510(4)−3.859(4) Å. To examine the correlation between the luminescence and intermolecular Pt(II)···Pt(II) interactions, solid-state luminescence measurements at room temperature and at 77 K have been carried out. Red-shifts in emission energies from room temperature to 77 K were observed for all complexes, and the cooling effect led to red-shifts of 310−550 cm^{-1} for the *anti* isomers and of 190−1260 cm^{-1} for the *syn* isomers. Thus, there is no obvious correlation between their emission energies and intermolecular Pt(II)···Pt(II) interactions. This can also be evidenced by the fact that **1b**, having the largest red-shift (1260 cm^{-1}), contains the longest intermolecular contact (3.859(4) Å) and **3**, having the smallest red-shift (190 cm^{-1}), contains the shortest intermolecular one (3.510(4) Å) for the *syn* isomers. In fact, the complexes with larger red-shifts of 1260 (**1b**) and 840 cm^{-1} (**2b**) are in parallel with their increased intermolecular $\pi\cdots\pi$ interactions. To clarify if the intermolecular $\pi\cdots\pi$ interactions instead of Pt(II)···Pt(II) ones are really responsible for the luminescence, the glass luminescence at 77 K and their concentration-dependence measurements were performed. Along with the red-shifts for the solid-state luminescence, which is temperature-dependence, the glass luminescence results further support that intermolecular $\pi\cdots\pi$ interactions instead of Pt(II)···Pt(II) ones are most likely correlated with the solid-state luminescence. Although our theoretical calculations suggest that intermoleculatr Pt(II)···Pt(II) interactions may be involved in the excited states, only the significant Pt(II)···Pt(II) interaction (i.e., 3.384(1) Å in *syn*-$[Pt(bpy)(NS)]_2(PF_6)_2$) plays an important role in the excited state, namely MMLCT instead of LLCT.

Acknowledgment. We thank the National Science Council and National Chung Cheng University of Taiwan for financial support and the National Center for High-performance Computer of Taiwan for computer resources.

Supporting Information Available: Schemes showing the syntheses of **2a**, **2b**, **3**, **4a**, and **4b**; ^{1}H NMR spectra for **1a**, **1b**, **2a**, **2b**, **3**, and **4b**; structures of **2a**, **2b**, **3**, and **4b**; solid-state emission spectra of **2a**, **2b**, and **3**; HOMO and LUMO diagrams of **1b**, **2b**, **3**, and syn-$[Pt(bpy)(NS)]_2(PF_6)_2$; absorption spectra of **1a** and **1b**; and cif data. This material is available free of charge via the Internet at http://pubs.acs.org.

References

(1) (a) Miskowski, V. M.; Houlding, V. H. *Coord. Chem. Rev.* **1991**, *111*, 145. (b) Miskowski, V. M.; Houlding, V. H.; Che, C.-M.; Wang, Y. *Inorg. Chem.* **1993**, *32*, 2518. (c) Brooks, J.; Babayan, Y.; Lamansky, S.; Djurovich, P. I.; Tsyba, I.; Bau, R.; Thompson, M. E. *Inorg. Chem.* **2002**, *41*, 3055. (d) Ma, B.; Li, J.; Djurovich, P.; Yousufuddin, M.; Bau, R.; Thompson, M. E. *J. Am. Chem. Soc.* **2005**, *127*, 28. (e) Yam, V. W.-W. *Acc. Chem. Res.* **2002**, *35*, 555. (f) Wong, K. M.-C.; Yam, V. W.-W. *Coord. Chem. Rev.* **2007**, *251*, 2477. (g) Lu, W.; Chan, M. C. W.; Zhu, N.; Che, C.-M.; Li, C.; Hui, Z. *J. Am. Chem. Soc.* **2004**, *126*, 7639. (h) Zhu, M. X.; Lu, W.; Zhu, N.; Che, C.-M. *Chem.—Eur. J.* **2008**, *14*, 9736. (i) Ibrahim Eryazici, I.; Moorefield, C N.; Newkome, G. R. *Chem. Rev.* **2008**, *108*, 1834.

(2) Krogmann, K. *Angew. Chem., Int. Ed. Engl.* **1969**, *8*, 35.

(3) *Extended Linear Chain Compounds*; Miller, J. S., Ed.; Plenum Press: New York, 1982; Vols. 1−3.

(4) (a) Yip, H.-K.; Cheng, L.-K.; Cheung, K.-K.; Che, C.-M. *J. Chem. Soc., Dalton Trans.* **1993**, 2933. (b) Yip, H.-K.; Che, C.-M.; Zhou, Z.-Y.; Mak, T. C.-W. *J. Chem. Soc., Chem. Commun.* **1992**, 1369.

(5) (a) Chan, C.-W.; Lai, T.-F.; Che, C.-M.; Peng, S.-M. *J. Am. Chem. Soc.* **1993**, *115*, 11245. (b) Chan, C.-W.; Cheng, L.-K.; Che, C.-M. *Coord. Chem. Rev.* **1994**, *132*, 87. (c) Wan, K.-T.; Che, C.-M.; Cho, K.-C. *J. Chem. Soc., Dalton Trans.* **1991**, 1077. (d) Kunkely, H.; Vogler, A. *J. Am. Chem. Soc.* **1990**, *112*, 5625.

(6) (a) Exstrom, C. L.; Sowa, J. R., Jr.; Daws, C. A.; Janzen, D.; Moore, G. A.; Stewart, F. F.; Mann, K. R. *Chem. Mater.* **1995**, *7*, 15. (b) Daws, C. A.; Exstrom, C. L.; Sowa, J. R., Jr.; Mann, K. R. *Chem. Mater.* **1997**, *9*, 363. (c) Buss, C. E.; Mann, K. R. *J. Am. Chem. Soc.* **2002**, *124*, 1031.

(7) (a) Truesdell, K. A.; Crosby, G A. *J. Am. Chem. Soc.* **1985**, *107*, 1787. (b) Crosby, G. A.; Highland, R. G.; Truesdell, K. A. *Coord. Chem. Rev.* **1985**, *64*, 41.

(8) (a) Vogler, A.; Kunkely, H. *J. Am. Chem. Soc.* **1981**, *103*, 1559. (b) Vogler, A.; Kunkely, H. *J. Am. Chem. Soc.* **1990**, *112*, 5625. (c) Paw, W.; Lachicotte, R. J.; Eisenberg, R. *Inorg. Chem.* **1998**, *37*, 4139. (d) Cummings, S. D.; Eisenberg, R. *J. Am. Chem. Soc.* **1996**, *118*, 1949. (e) Cummings, S. D.; Eisenberg, R. *Inorg. Chem.* **1995**, *34*, 2007. (f) Bevilacqua, J. M.; Eisenberg, R. *Inorg. Chem.* **1994**, *33*, 2913. (g) Bevilacqua, J. M.; Zuleta, J. A.; Eisenberg, R. *Inorg. Chem.* **1993**, *32*, 3689. (h) Zuleta, J. A.; Bevilacqua, J. M.; Eisenberg, R. *Coord. Chem. Rev.* **1992**, *111*, 237.

(9) Tzeng, B.-C.; Fu, W.-F.; Che, C.-M.; Chao, H.-Y.; Cheung, K.-K.; Peng, S.-M. *J. Chem. Soc., Dalton Trans.* **1999**, 1017.

(10) (a) Kato, M.; Omura, A.; Toshikawa, A.; Kishi, S.; Sugimoto, Y. *Angew. Chem., Int. Ed.* **2002**, *41*, 3183. (b) Kato, M. *Bull. Chem. Soc. Jpn.* **2007**, *80*, 287.

(11) (a) Moulton, B.; Zaworotko, M. *J. Chem. Rev.* **2001**, *101*, 1629. (b) Peng, R.; Deng, S. R.; Li, M.; Li, D.; Li, Z. Y. *CrystEngComm* **2008**, *10*, 590.

(12) Mann, F. G.; Watson, H. R. *J. Chem. Soc.* **1958**, 2772.

(13) (a) *SMART V5.625 Software for the CCD Detector System*; Bruker-axs Instruments Division: Madison, WI, 2000. (b) *SAINT V6.22 Software for the CCD Detector System*; Bruker-axs Instruments Division: Madison, WI, 2000. (c) Sheldrick, G. M. *SADABS, V 2.03*; University of Göttingen: Germany, 2002. (d) Sheldrick, G. M. SHELXS-97. *Acta. Crystallogr.* **1990**, *A46*, 467. (e) Sheldrick, G. M. *SHELXL-97*; University of Göttingen: Germany, 1997.

(14) (a) Becke, A. D. *J. Chem. Phys.* **1993**, *98*, 5648. (b) Lee, C.; Yang, W.; Parr, R. G. *Phys. Rev. B* **1988**, *37*, 785. (c) Hay, P. J.; Wadt, W. R. *J. Chem. Phys.* **1985**, *82*, 299.

(15) Frisch, M. J. et al. *Gaussian 03*, Revision E.01; Gaussian, Inc.: Wallingford, CT, 2004.

(16) Umakoshi, K.; Kinoshita, I.; Fukui-Yasuba, Y.; Matsumoto, K.; Ooi, S.; Nakai, H.; Shiro, M. *J. Chem. Soc., Dalton Trans.* **1989**, 815.

(17) Roundhill, D. M.; Gray, H. B.; Che, C.-M. *Acc. Chem. Res.* **1989**, *22*, 55.

(18) Burke, J. M.; Fackler, J. P., Jr. *Inorg. Chem.* **1972**, *11*, 3000.

(19) Osborn, R. S.; Rogers, D. *J. Chem. Soc., Dalton Trans.* **1974**, 1002.

(20) Janiak, C. *J. Chem. Soc., Dalton Trans.* **2000**, 3885.